Impact of Si doping on radio frequency dispersion in unpassivated GaN/AlGaN/GaN high-electron-mobility transistors grown by plasma-assisted molecular-beam epitaxy

Oleg Mitrofanov, Michael Manfra, and Nils Weimann

Citation: Appl. Phys. Lett. **82**, 4361 (2003); doi: 10.1063/1.1582373
View online: http://dx.doi.org/10.1063/1.1582373
View Table of Contents: http://apl.aip.org/resource/1/APPLAB/v82/i24
Published by the American Institute of Physics.

Impact of Si doping on radio frequency dispersion in unpassivated GaN/AlGaN/GaN high-electron-mobility transistors grown by plasma-assisted molecular-beam epitaxy

Oleg Mitrofanov,[a] Michael Manfra, and Nils Weimann
Bell Laboratories, Lucent Technologies, 600 Mountain Avenue, Murray Hill, New Jersey 07974

(Received 31 March 2003; accepted 14 April 2003)

We report on the effect of Si doping on the transient behavior of unpassivated high-power GaN/AlGaN/GaN high-electron-mobility transistors grown by plasma-assisted molecular-beam epitaxy on 6H–SiC. The incorporation of Si into the heterostructure barrier is found to reduce the level of radio frequency dispersion as compared to undoped structures. In some devices which incorporate Si doping of the barrier, the pulsed and steady-state current–voltage characteristics coincide, and gate lag is found to be insignificant. More typically, ~90% of the dc value of drain current is restored at 1 μs after pulsing the gate from pinch off to $V_{GS}=0$ V. Significant gate lag is observed in devices that are not doped with Si. In the undoped structure, the drain current reaches only ~70% of the dc value within 1 μs. The transient behavior in the two designs is attributed to the same defect state with activation energy of 0.22 eV. Dispersion reduction is correlated with an increase of gate leakage current in Si-doped devices. © *2003 American Institute of Physics.*
[DOI: 10.1063/1.1582373]

Recent advances in the development of AlGaN/GaN high-electron-mobility transistors (HEMTs) has led to the demonstration of power densities exceeding 10 W/mm at 8 GHz[1,2] and 5 W/mm at 26 GHz for small periphery devices.[3] Nevertheless, significant radio frequency (rf) dispersion is still observed in many devices, which represents a significant challenge to future progress. rf dispersion is characterized by an increase of the knee voltage and a drop in the maximum channel current at microwave frequencies. Several groups have shown that the effects of dispersion can be mitigated in metalorganic chemical vapor deposition grown epilayers by passivating the device surface with SiN.[1,2,4–6] More recently, SiN passivation has been used to improve molecular-beam epitaxy (MBE) grown layers as well.[7] These results strongly suggest that surface state traps are responsible for dispersion. However, the specific trap states involved in rf dispersion are neither well known, nor are the physical mechanisms by which SiN passivation reduces the effect.

Moon *et al.*[8] have reported excellent power performance for unpassivated AlGaN/GaN HEMTs grown by MBE. We have recently demonstrated GaN/AlGaN/GaN HEMTs grown by plasma-assisted MBE on 6H–SiC with power densities exceeding 8 W/mm at 2 GHz (Ref. 9) and 6 W/mm at 7 GHz (Ref. 10) achieved without surface passivation. These results suggest that dispersion effects can be minimized with proper structure design and control of MBE growth conditions.

In this letter, we report on the characterization of transient behavior of unpassivated GaN/AlGaN/GaN HEMTs grown by MBE. We discuss the role of Si doping of the barrier in the HEMT structure. Measurements of pulsed current–voltage ($I-V$) curves and gate lag are used to quantify the temporal response of the device and to help identify physical processes that result in rf dispersion.

We compare the dispersion observed in two heterostructure designs. The epilayers differ only in the doping of the AlGaN barrier and GaN capping layer. In both structures, a 60 nm thick AlN nucleation layer is deposited on semi-insulating 6H–SiC. The nucleation layer is grown at a substrate temperature of 800 °C. The nucleation layer is followed by approximately 2 μm of undoped GaN grown at 0.5 μm/h with a Ga flux just below the transition to Ga droplet formation. The substrate temperature is 745 °C. The GaN buffer is followed with a 30 nm thick $Al_{0.34}Ga_{0.66}N$ barrier and the heterostructure is completed with a 5 nm GaN capping layer. The substrate temperature is not changed during the deposition of the barrier structure. In the first design, the upper 15 nm of the AlGaN barrier and the 5 nm GaN capping layer are doped with Si at a level of 1×10^{18} cm^{-3}. The second design does not incorporate any Si doping.

Devices are fabricated from these epilayers using optical contact lithography. After dry etch mesa isolation, ohmic contacts were defined with a drain–source opening of 5 μm. The Ti/Al/Ni/Au ohmic metal stack was alloyed at 850 °C in N_2 atmosphere. Lastly, 1 μm long Schottky gates were deposited by electron-beam evaporation of Ni (300 Å) followed by Au (3000 Å). The chips were not passivated before measurement. The devices are laid out in coplanar test frames in common-source configuration for on-wafer testing. Each HEMT consists of two opposed gate fingers, with total gate periphery of 50 μm. dc device characteristics were measured on wafer with an HP4145B parameter analyzer using needle probes. For transient characterization, the gate potential was controlled with a pulse generator. The gate voltage is pulsed from pinch off to $V_{GS}=0$ V. The pulse rise and fall time is 150 ns. The transient drain current is measured using a low insertion impedance current probe and displayed on a digitizing oscilloscope.

[a]Electronic mail: olegm@lucent.com

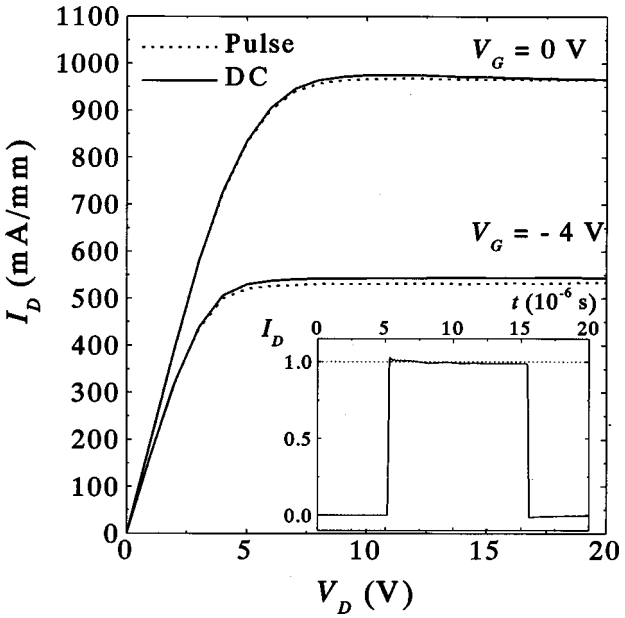

FIG. 1. Pulsed and steady-state $I-V$ characteristics of a device that displays minimal dispersion. The inset shows the response of the drain current to a 10 μs gate pulse. The gate is pulsed from pinch off $V_{GS}=-10$ V to $V_{GS}=0$ V with duty cycle of 0.1%; the drain is biased in saturation at $V_{DS}=10$ V.

The temporal response of a Si-doped heterostructure that displays minimal dispersion is shown in Fig. 1. The inset displays the drain current response to a 10 μs gate pulse from $V_{GS}=-10$ V to $V_{GS}=0$ V with a duty cycle of 0.1%. During most of the measurement, the device is stressed in the off state (-10 V). The transistor switches to the full dc current value within 100–200 ns (limited by the temporal resolution of the measurement setup). The pulsed $I-V$ characteristics using a 10 μs pulse are compared to the steady-state $I-V$ characteristics in Fig. 1. Large signal load pull measurements of devices that display similar characteristics have yielded power densities over 8 W/mm at 2 GHz. The measured saturated power density in these devices agrees with the value predicted from a simple load-line analysis of the dc $I-V$ characteristics. In the course of this study, we have evaluated several wafers that incorporate Si doping of the barrier. The behavior shown in Fig. 1 represents the devices displaying the least dispersion. In Si-doped devices, as discussed next, we typically observed an approximately 90% recovery of drain current in 1 μs after pulsing the gate from pinch off to $V_{GS}=0$ V.

In order to present a statistically significant comparison of gate lag between the undoped and doped designs, we compare 15 devices from both one doped and one undoped wafer. The Si-doped structure exhibited a room-temperature mobility of 1300 $cm^2/V\,s$ with a sheet density of 1.3×10^{13} cm^{-2}. The mobility of the undoped structure was 1400 $cm^2/V\,s$ with a sheet density of 1.1×10^{13} cm^{-2} at room temperature.

The gate-lag measurements are performed in a common source configuration. The transistors are biased into saturation. The gate voltage is pulsed from pinch off to $V_{GS}=0$ V for a duration of 15 μs with a duty cycle of 0.15%. Figure 2 compares the temporal response of the drain current in a Si-doped and an undoped device. The plotted results are two individual scans that reside close to the average behavior

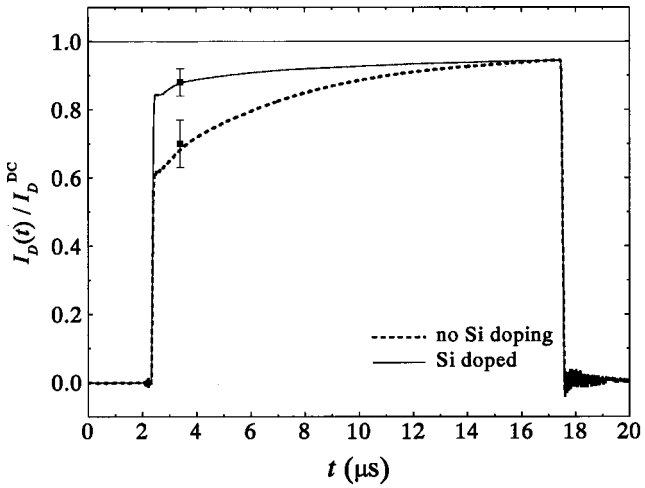

FIG. 2. Typical gate lag in the Si-doped and undoped devices. The error bars indicate the standard deviation of the drain current at $t=1$ μs in the ensemble of 15 devices of each design. The gate is pulsed from pinch off (Si doped: $V_{GS}=-10$ V; undoped: $V_{GS}=-11$ V) to $V_{GS}=0$ V with duty cycle of 0.15%; the drain is biased in saturation at $V_{DS}=15$ V.

observed in each design. The recovery in each case is normalized to the steady-state current value at $V_{GS}=0$ V. For the 15 undoped devices, the average recovery after 1 μs is 70 $\pm$7%. The doped devices show an average recovery after 1 μs of 88$\pm$4%. The standard deviation from the average value at 1 μs is indicated by the error bar. Based on this analysis, it is clear that the Si doping has reduced the amount of dispersion seen relative to the undoped case.

The dynamics of current recovery in the doped and undoped samples have similar features. As the gate voltage switches from the pinch off to the open channel state, the drain current instantaneously rises to an initial level (following the 150 ns gate pulse rise time). In the case of the Si-doped devices, the initial level is 85$\pm$5% while it is only 64$\pm$6% for the undoped devices. The initial step is followed by 10–15 μs nonexponential recovery which crosses over into an exponential approach to the steady-state current value. Figure 3 shows the transient characteristics of an undoped device. The time constant of the exponential approach is $\sim$50 μs at room temperature. The similarity in the

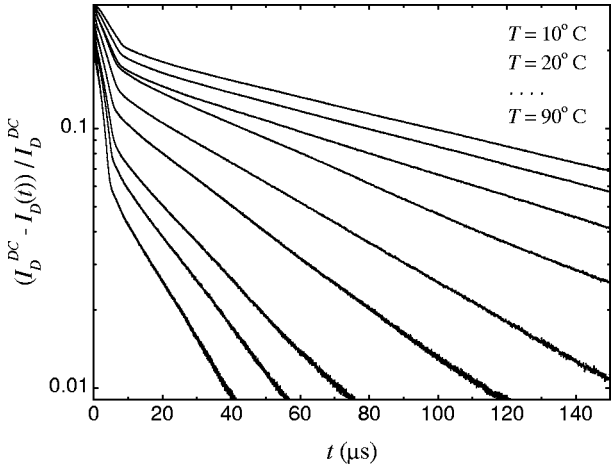

FIG. 3. Transient drain current measured in undoped devices at temperatures ranging from 10 to 90 °C. The gate is pulsed from pinch off $V_{GS}=-11$ V to $V_{GS}=0$ V; the drain is biased in saturation at $V_{DS}=12$ V.

qualitative transient characteristics of the doped and undoped devices suggests that the same physical process is responsible for the rf dispersion. However, a significantly smaller effect observed in the doped devices implies that Si incorporation into the barrier facilitates the drain current recovery process.

Not surprisingly, the amount of gate leakage is also changed by the Si doping of the AlGaN barrier and the GaN capping layer. The average gate leakage measured in the undoped devices was 65 μA/mm at gate to drain bias of $V_{GD}=-25$ V. The doped devices displayed much higher gate leakage. The average value for the doped devices was 480 μA/mm at a gate to drain bias of -25 V.

At this point, the physics of gate lag reduction in the doped devices is not completely clear. The higher leakage current indicates that a weak conduction channel is formed near the surface of the structure. The channel can be associated with lowering of the conduction band level relative to the Fermi level in the GaN cap layer due to the presence of Si donors and with the Si-site assisted conduction. As noted herein, the rf dispersion in AlGaN/GaN HEMTs is at least partially related to active electronic states on the surface. The effect of the surface charging will be reduced in the system with the weak conduction channel near the surface, which can screen the two-dimensional electron gas from the active surface states.

In order to further our understanding of the defect states involved in dispersion in GaN/AlGaN/GaN heterostructures, we have investigated the kinetic behavior of the active states. The response of the channel current to the gate potential depends on the operating temperature. A series of transients measured on the undoped device at temperatures between 10 °C and 90 °C is shown in Fig. 3. The initial level of the current response increases at the elevated temperatures, and the consequent approach to the steady-state level becomes faster. The rate constant τ^{-1} extracted from fitting the function $I_D(t)=I_D^{dc}(1-I_0\exp[-t/\tau])$ to the exponential portion of the transient data is plotted in Fig. 4 as a function of the inverse temperature. The temperature dependence of the process follows the classical kinetic behavior of the Arrhenius equation $\tau^{-1}=CT^2\exp(-E_A/kT)$. The activation energy E_A of the process was found to be 0.22 ± 0.01 eV. The electronic state associated with this activation energy is only one of the active states that potentially influence dispersion in GaN/AlGaN/GaN HEMTs. A more detailed study of the transient characteristics is underway to fully understand the complex behavior of the dispersion.

In conclusion, we investigated the effects of Si doping on the dispersion in unpassivated. GaN/AlGaN/GaN HEMTs grown by plasma-assisted MBE. The incorporation of Si in the heterostructure barrier is found to reduce the level of rf dispersion, and in some cases, remove it entirely. Study of the transient behavior showed qualitatively similar characteristics in the doped and undoped devices. Investigation of the temperature dependence of gate lag yielded at least one thermally activated electronic state with energy of 0.22 eV.

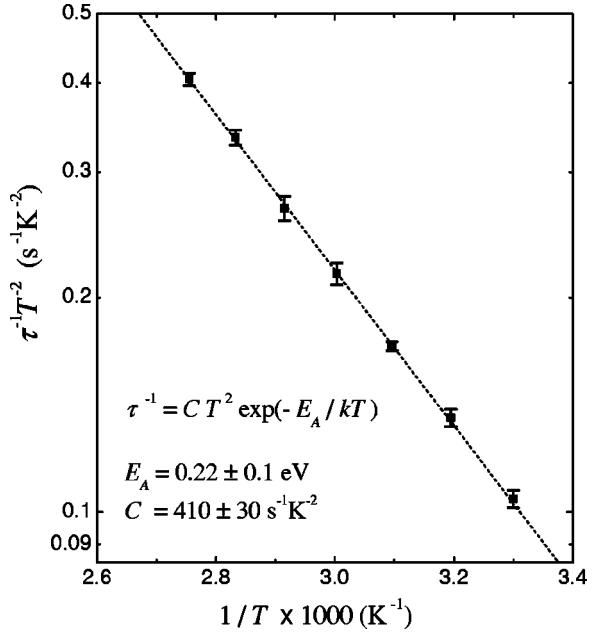

FIG. 4. Temperature dependence of the rate constant extracted from the data in Fig. 3.

[1] U. Mishra, P. Parikh, and Y.-F. Wu, Proc. IEEE **90**, 1022 (2002).
[2] V. Tilak, B. Green, V. Kaper, H. Kim, T. Prunty, J. Smart, J. Shealy, and L. Eastman, IEEE Electron Device Lett. **22**, 504 (2001).
[3] C. Lee, H. Wang, J. Yang, L. Witkowski, M. Muir, M. A. Khan, and P. Saunier, Electron. Lett. **38**, 924 (2002).
[4] B. M. Green, K. K. Chu, E. Martin Chumbes, J. A. Smart, J. R. Shealy, and L. F. Eastman, IEEE Electron Device Lett. **21**, 268 (1999).
[5] R. Ventury, N. Q. Zhang, S. Keller, and U. K. Mishra, IEEE Trans. Electron Devices **48**, 560 (2001).
[6] S. C. Binari, P. B. Klein, and T. E. Kazior, Proc. IEEE **90**, 1048 (2002).
[7] D. S. Katzer, S. C. Binari, D. F. Storm, J. A. Roussos, B. V. Shanabrook, and E. R. Glaser, Electron. Lett. **38**, 1740 (2002).
[8] J. S. Moon, M. Micovic, P. Janke, P. Hashimoto, W. S. Wong, R. D. Widman, L. McCray, A. Kurdoghlian, and C. Nguyen, Electron. Lett. **37**, 528 (2001).
[9] N. G. Weimann, M. J. Manfra, and T. Wachtler, IEEE Electron Device Lett. **24**, 57 (2003).
[10] M. J. Manfra and N. G. Weimann, Proceedings of the 2002 Fall Meeting of the Materials Research Society, 2–6 December 2002, Boston, MA.